Nanoscale

PAPER

View Article Online
View Journal | View Issue

Cite this: *Nanoscale*, 2016, **8**, 12553

Stimuli-free programmable drug release for combination chemo-therapy†

Li Fan,[a,b] Boquan Jin,[c] Silu Zhang,[b] Chaojun Song*[c] and Quan Li*[b]

Received 13th September 2015,
Accepted 27th October 2015

DOI: 10.1039/c5nr06305a

www.rsc.org/nanoscale

Combinational chemotherapy capable of targeted delivery and programmable multi-drug release leads to enhanced drug efficacy, and is highly desired for cancer treatment. However, effective approaches for achieving both features in a single treatment are limited. In the present work, we demonstrated programmed delivery of both chemotherapeutic and immunotherapeutic agents with tumor cell targeting capability by using SiO_2 based self-decomposable nanoparticulate systems. The programmable drug delivery is realized by manipulating drug loading configurations instead of relying on external stimuli. Both *in vitro* and *in vivo* results showed specific drug binding to FAT1-expressing colon cancer cells. The loaded dual drugs were demonstrated to be delivered in a sequential manner with specific time intervals between their peak releases, which maximize the synergistic effect of the chemotherapeutics. These features led to significantly enhanced drug efficacy and reduced system toxicity. The tumor weight decreased by 1/350, together with a moderate increase in rats' body weight, which were observed when adopting the dual drug loaded nanoparticles, as compared to those of the control groups. The present system provides a simple and feasible method for the design of targeting and combination chemotherapy with programmed drug release.

Introduction

Combination chemotherapy has long been adopted in clinics as a primary cancer treatment regimen.[1,2] It has been demonstrated that the multiple-drug "cocktail treatment" may function synergistically for higher therapeutic efficacy.[3] Nevertheless, the free drug "cocktail treatment" is found to be associated with a significantly increased adverse effect, which explains the little increase in the median survival time,[1] despite its higher therapeutic efficacy. A nanoparticle carrier is capable of loading multiple cargos with different functionalities,[4,5] and thus provides an ideal platform to carry out the "cocktail treatment" with possibly reduced toxic effects. However, in many cases the "cocktail treatment" requires that chemotherapy agents be programmed into a specific release pattern, *e.g.*, sequentially release individual agents at required time points, in order to achieve the best antitumor efficacy. The existing programmable systems require multiple triggers incorporated in the drug carrier in order to activate the drug release, and the programmed release relies on the availability of external stimuli, limiting the application of such systems.[6–8] A multi-cargo loaded drug carrier system with a programmable drug release function that does not rely on external stimulus becomes an attractive alternative.

On the other hand, lack of selectivity in most of the therapeutic agents is also a major limitation, which results in significant toxicity to normal cells.[9] Although the enhanced permeability and retention (EPR) effect passively serves as a targeting strategy in the case of nanoparticle delivery systems, active targeting by attaching target-specific ligands to the surface of nanoparticles[10–13] is necessary to improve the cancer-specific selectivity. As a result, when considering the limited space available, adequate loading of both the targeting agent and multiple therapeutic components into a single nanocarrier becomes challenging, especially when an additional agent for improved NP biocompatibility also needs to be taken into consideration.[14,15]

In the present work, we have realized sequential delivery of chemotherapeutics with a specific time lag in-between the peak releases of individual drugs. This is achieved by dual-loading of a self-decomposable nanoparticle system (Fig. 1a). The specific release pattern is determined by drug loading configurations instead of relying on external stimuli. Dox is the most widely used chemotherapeutic agent and is generally prescribed in combination with other drugs. Methylene blue (MB)

[a]*Department of pharmaceutical analysis, School of Pharmacy, The Fourth military medical university, Xi'an, Shaanxi, China 710032*
[b]*Department of Physics, The Chinese University of Hong Kong, Shatin, New Territories, Hong Kong, China. E-mail: cj6005@fmmu.edu.cn*
[c]*Department of Immunology, Fourth military medical university, Xi'an, Shaanxi, China 710032. E-mail: liquan@phy.cuhk.edu.hk*
†Electronic supplementary information (ESI) available. See DOI: 10.1039/c5nr06305a

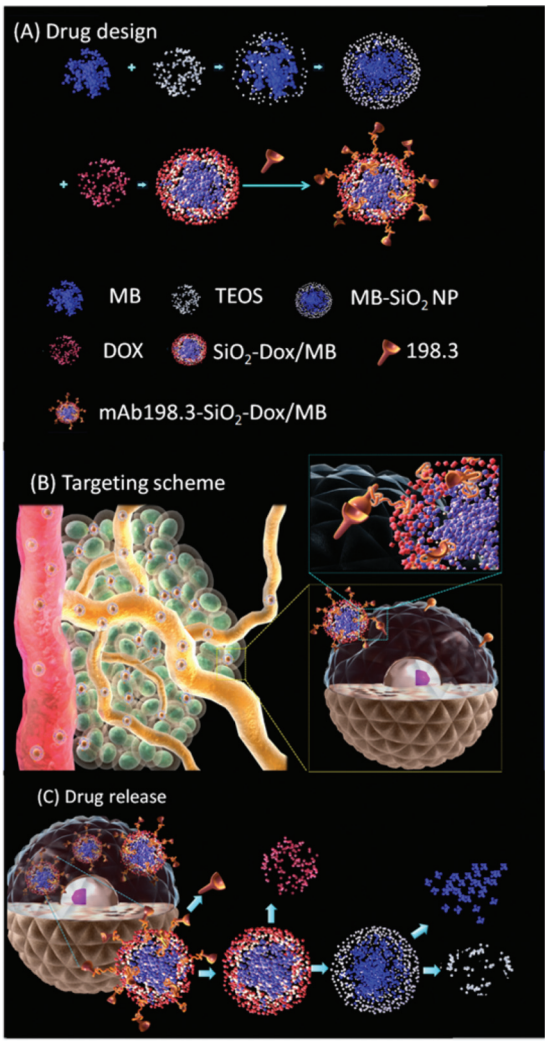

Fig. 1 Schematic illustration showing the design of the SiO_2NP delivery system, its targeting, and sequential drug delivery process. (a) Configuration of the mAb198.3-SiO_2-Dox/MB NP drug, (b) targeting of the NP drug *via* binding to FAT1-expressing cells, (c) multi-drug release process in a sequential manner.

is also a common drug for clinical use in methemoglobinemia, Barrett's esophagus, cervical cancer, and traumatic knee arthrotomy, and photodynamic therapy.[16–21] MB has another therapeutic feature, *i.e.*, MB has been found to serve as a sensitizer for Dox.[22] This inspired our present work on dual loading the NP carriers with both Dox and MB, with the latter serving as the sensitizer for the former. Then by surface decorating such dual-loaded nanoparticles with mAb198.3 (Fig. 1a), which serves as both the targeting agent and the immunotherapeutic, we demonstrated significantly enhanced drug efficacy and reduced system toxicity. The "all-in-one" nanoparticle system features the function of cancer specific targeting (Fig. 1b), multi-modalities with both immuno- and chemo-therapeutic agents, and sequential delivery of the chemotherapeutics (Fig. 1c). Such a nanodrug (nanocarrier loaded with a drug and surface decorated with specific functional groups) (Fig. 1) was found to specifically bind to FAT1-expressing colon cancer cell lines with easy cellular internalization. After that, the dual-loaded chemotherapeutics were released in a sequential manner with an ~12 h-interval in their peak concentration. All these factors contribute to the significantly enhanced drug efficacy and reduced system toxicity. The present system provides simple and feasible strategies for the design of anticancer drug and/or other delivery systems that require a programmed cargo release.

Results and discussion

SiO_2-Dox/MB NPs were synthesized with MB being concentrated in the middle of the nanoparticle, and Dox being located mostly in the surface/subsurface layers. Dox was absorbed by electrostatic interaction, as it itself is positively charged and the SiO_2 NPs are negatively charged. Such a configuration was obtained by growing MB molecules together with the silica species,[23] and absorbing Dox onto the MB-SiO_2 NPs afterwards (Fig. 1a). These NPs were spherical with an average diameter of ~100 nm and a size range of 80–120 nm (Fig. 2a). Both MB and Dox were successfully loaded into the NPs, as suggested by UV-Vis absorption spectra taken at different stages of the loading processes (Fig. 2b). The "grown-in" MB in the NPs shows absorption peaks at ~600 nm, matching that of pure MB. When Dox was loaded, an additional absorption peak in the range of 400–600 nm confirmed the

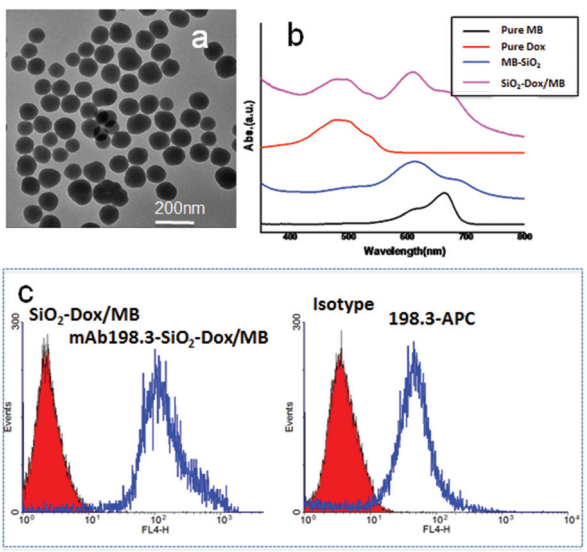

Fig. 2 Characterization of the mAb198.3-SiO_2-Dox/MB NPs. (a) TEM image taken from the SiO_2-Dox/MB NPs showing their morphology and sizes characterized by TEM. (b) UV-Vis absorption spectra taken at different stages of the loading process. (c) Flow cytometry analysis showing the binding capability of mAb198.3-SiO_2-Dox/MB NP system to native FAT1 molecules on the surface of Colo205 cells. The *x*-axis represented the fluorescence intensity of the APC dye (c right) or MB (c left). FL4-H represented the emission collected using a channel of 650–750 nm, when being excited at 633 nm.

presence of Dox in the sample. Drug encapsulation/loading capabilities have been evaluated by a UV-Vis spectrum.

Surface decoration of the NPs with mAb198.3 (mAb198.3-SiO_2-Dox/MB NPs) did not affect their shape and morphology. The successful attachment of mAb198.3 to NPs was confirmed by sodium dodecyl sulphate-polyacrylamide gel-electrophoresis (SDS-PAGE). MAb198.3-SiO_2-Dox/MB NPs showed bands at 50 kDa (heavy chain) and 25 kDa (light chain), which was consistent with the free mAb198.3 groups (Fig. SI1†). MAb198.3 is a recently generated monoclonal antibody (mAb). It can recognize the FAT1 protein in Colorectal Cancer (CRC) and be rapidly internalized when it binds to FAT1-expressing colon cell lines.[25] Compared to the APC dye labelled isotype (similar to mAb as mAb198.3 but without a specific binding capability toward colo-205 cells), the strong binding affinity of mAb198.3 (APC dye labelled) to the Colo205 cells was revealed by the florescence intensity increase (positive rate of 97.11%) in the flow cytometry data, which resulted from the larger population of the APC dye per cell (Fig. 2c right). On testing the mAb198.3-SiO_2-Dox/MB nanoparticle system, the encapsulated MB took a similar role as that of the APC dye (both MB and APC can be excited at 633 nm and their emission was collected at 650–750 nm). The flow cytometry results of mAb198.3-SiO_2-Dox/MB NPs also show a considerable fluorescence intensity increase (positive rate of 98.38%), when compared to that of SiO_2-Dox/MB NPs (Fig. 2c left), suggesting both the successful attachment of mAb198.3 to the NPs and NPs' capability of FAT1 binding. The release of the multi-drugs from the mAb198.3-SiO_2-Dox/MB NPs was designed to take place in subsequent stages after their endocytosis process. MAb198.3, serving as both targeting ligands and immunotherapeutics, would be the first ones to carry out their anti-cancer functions after being internalized. After that, Dox and MB would be released in a sequential manner known as the second (Dox release dominant) and the third stages (MB release dominant).

For *in vitro* experiments, both Dox and MB concentrations were fixed at 0.5μg ml^{-1}, which was chosen based on the MTT results (Fig. SI2†). At this concentration, the cells fed with pure Dox or pure MB showed a vitality value of ~73%, and ~91%, respectively. Although MB itself has low cytotoxicity especially at low concentrations,[24] it had been found that co-administration of MB with Dox increased the cytotoxicity of the latter in cancer cells, and an ~12 h time lag between the peak release of the two gives the best efficacy enhancement *in vitro* (Fig. SI3†), *i.e.*, the cell viability dropped from ~69% for the simultaneous administration of Dox and MB to ~40% when there is a time lag of 12 h between them (Dox first, followed by MB after 12 h.).

In order to achieve the desired sequential release pattern of the drugs when employing the NP carriers (*i.e.*, 12 h time lag between the peak release of Dox and MB), we identified the suitable ratio between MB and Dox in the nanoparticle carrier, which was found to affect the time lag between the two peak-releases (Fig. SI4†).

As shown in Fig. 3, a MB/Dox ratio of 1 gives the desired release profiles in colo 205 cells. This ratio was chosen to carry

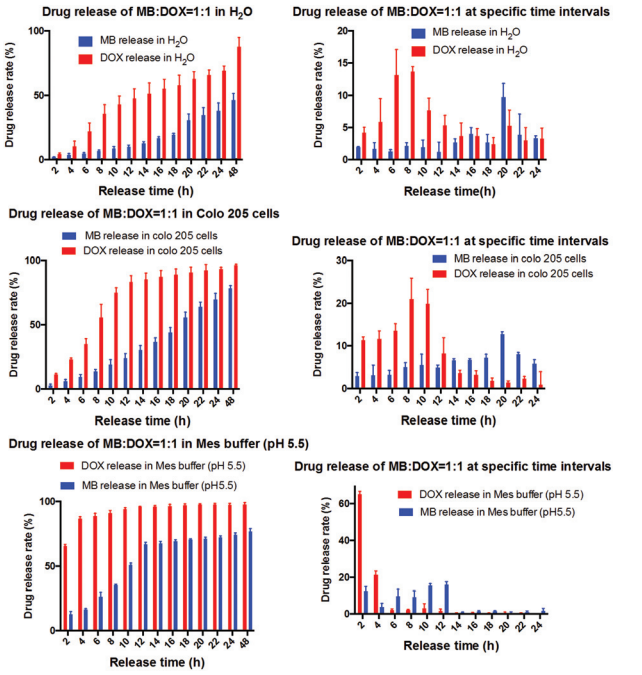

Fig. 3 The cumulative drug release profiles and those plotted at specific time intervals (every 2 h) in H_2O, Colo 205 cells, and Mes buffer (pH 5.5).

out the following *in vitro* and *in vivo* experiments. The release profiles of the mAb198.3-SiO_2-Dox/MB NPs were examined in DI water, in colo-205 cells, and in Mes buffer (pH 5.5, at 37 °C, simulating lysosome pH environment). UV absorption spectra were taken from the respective supernatants to measure the amount of MB and Dox released at specific time points. Both the cumulative drug release profiles and those plotted at specific time points were shown in Fig. 3. When the NPs were dispersed in H_2O and in colo-205 cells, a quick initial rise in the amount of Dox appeared in the first ~8 h intervals, after that it leveled off. The release of MB came later, and it took ~20 h to reach the peak MB concentration. There is an ~12 h lag between the peak release of Dox and MB. The Dox and MB releases were found to be faster, when the NPs were dispersed in Mes buffer (pH 5.5), *i.e.*, an ~8 h time lag existed between the peak release of Dox and MB.

Along with the drug release from the nanoparticles, a morphological evolution of the mAb198.3-SiO_2-Dox/MB NPs was also observed (Fig. 4). Most of the NPs remained intact in the first few hours of drug release, after which obvious hollow features gradually appeared in the center of NPs. Further drug release coincided with the continuous enlargement of the NPs' hollow feature, and eventually fine fragmentation of the carrier appeared when drugs were completely released. This is a unique feature of the self-decomposable NPs.[23]

Now we discuss the efficacy of the mAb198.3-SiO_2-Dox/MB NPs. Fig. 5 compares the efficacy of pure Dox, pure MB, co-administration of Dox and MB, co-administration of Dox and MB with a 12 h time lag, SiO_2-Dox/MB NPs, and mAb198.3-

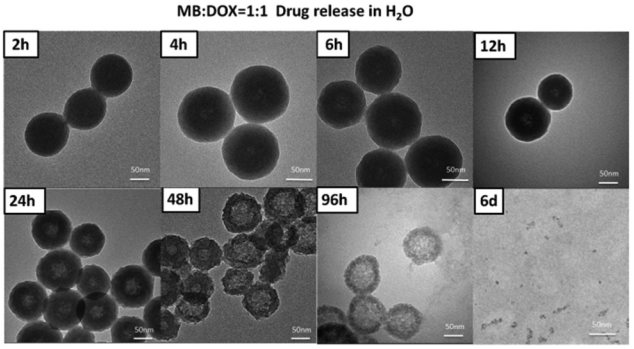

Fig. 4 Morphological evolution of the mAb198.3-SiO_2-Dox/MB NPs dispersed in H_2O was also observed by TEM from 2 h to 6 days.

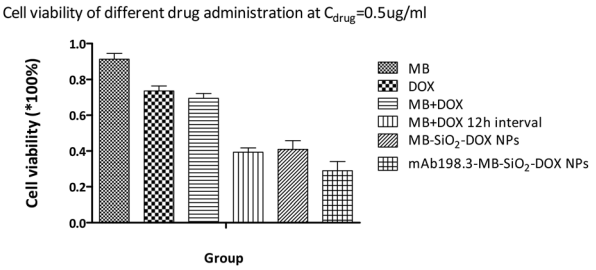

Fig. 5 Cell viability of pure MB, pure Dox, co-administration of Dox and MB, co-administration of Dox and MB with a 12 h time difference, SiO_2-Dox/MB NPs, and mAb198.3-SiO_2-Dox/MB NPs was investigated by the MTT assay. Both Dox and MB concentrations were fixed at 0.5 μg ml^{-1}.

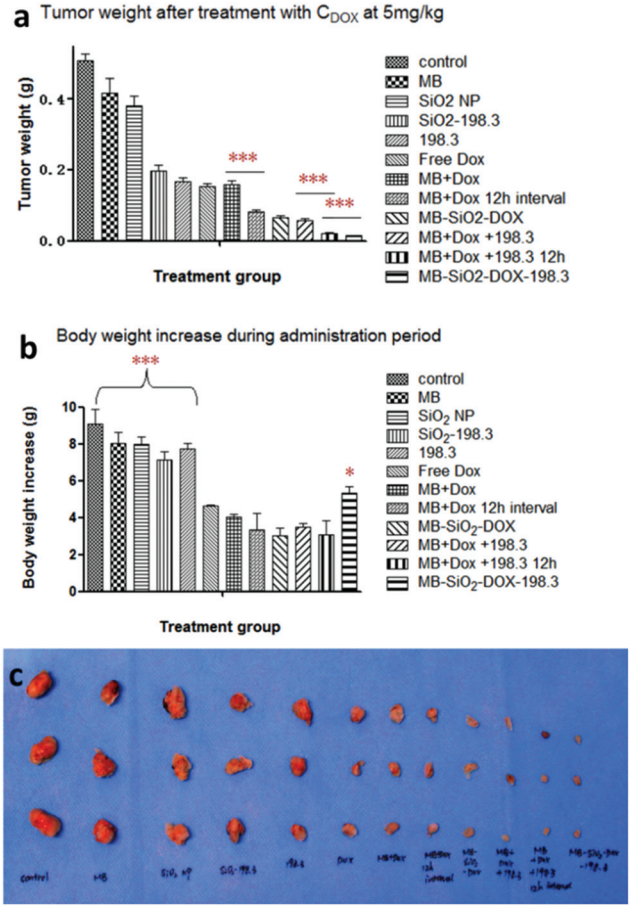

Fig. 6 Antitumor effect of mAb198.3-SiO_2-Dox/MB on nude mice bearing Colo-205 cells subcutaneously was studied *in vivo*. Values of tumor weight (a) and body weight changes (b) are expressed as mean ± SD (g, n = 5). Dissected tumor tissues from the nude mice (c). The nude mice were administered *via* i.v. injection every 3 days. *P < 0.05, ***P < 0.0001.

SiO_2-Dox/MB NPs (MB/Dox ratio of ~1). Co-administration of Dox and MB at the same time showed similar cytotoxicity as that of pure Dox (~69% viability). Nevertheless, when the administration of MB was carried out 12 h after that of Dox, the cell viability significantly dropped to ~40%. Similar results were found in the case of SiO_2-Dox/MB NPs. A further decrease in cell viability was obtained when mAb198.3-SiO_2-Dox/MB NPs were employed.

We then evaluated the antitumor efficacy of mAb198.3-SiO_2-Dox/MB NPs in a xenograft mouse model by intravenous (i.v.) injection. The nanoparticle drug significantly delayed subcutaneous colo-205 tumor growth, as demonstrated by the tumor weight at a dose of 5 mg kg^{-1} every three days (Fig. 6a and c). Delayed tumor growth was primarily ascribed to two factors, *i.e.*, targeted therapy due to the presence of mAb198.3 and synergistic effect originating from the programmed release of Dox and MB loaded in the nanoparticle carrier. The MB + Dox with 12 h interval administration group delayed tumor growth significantly, when compared with the MB + Dox co-administration group (P < 0.0001, analyzed by one-way ANOVA with Bonferroni's multiple comparison test). The tumor inhibitory rate of the SiO_2-Dox/MB treatment group is slightly higher than that on the co-administration of MB and Dox with a 12 h interval, but much higher than that of the groups treated with pure Dox or MB, or by co-administration of Dox and MB simultaneously. This is consistent with the *in vitro* findings. This result also demonstrated that co-delivery of MB and Dox using the self-decomposable SiO_2 NP system can maximize the synergistic effect of MB and Dox. The tumor inhibitory rate was further increased by introducing mAb198.3 into the NPs. The treatment group of MB + Dox + mAb198.3 with a 12 h interval between Dox and MB could significantly delay tumor growth when compared with co-administration simultaneously (P < 0.0001). At the last measurement point, the tumor weight decreased by 1/350 in the tumor samples treated with mAb198.3-SiO_2-Dox/MB when compared with the control group.

On the other hand, changes in body weights were also investigated to evaluate the system toxicity of mAb198.3-SiO_2-Dox/MB NPs (Fig. 6b and SI5†). The data were analyzed using GraphPad Prism 5.01® software using one-way ANOVA, and differences were considered statistically significant at P < 0.05. Treatment groups including free Dox, MB + Dox and MB + Dox 12 h interval, MB + Dox + mAb198.3, MB + Dox + mAb198.3

12 h interval and SiO_2-Dox/MB exhibited no significant differences in body weight increase ($P > 0.05$), indicating obvious system toxicity. Significant body weight increases were observed in the control group, the pure MB group, blank NP groups without chemotherapeutics, the pure mAb198.3 group, and NP groups with mAb198.3 only (no chemo agents) ($P < 0.0001$). As a comparison, a moderate increase in body weight was observed in the mAb198.3-SiO_2-Dox/MB treatment group ($P < 0.05$), which is much more significant than that of the groups treated with the same drugs (MB + Dox + mAb198.3 simultaneously or with a 12 h interval between MB and Dox) in the absence of NP carriers, indicating that using mAb198.3-SiO_2-Dox/MB NPs as delivery systems of multiple drugs could significantly decrease the system toxicity caused by combinational chemotherapy.

Experimental section

Synthesis and characterization of mAb198.3-SiO_2-Dox/MB sequential drug delivery system

The SiO_2-MB NPs were synthesized using a modified Stober method reported elsewhere.[23] Briefly, MB (2.5 mg) was dissolved in ethanol (75 mL) with ammonia–water solution (3.4 mL, 25%, v/v), followed by the addition of 80 μL TEOS. The SiO_2-MB NPs were obtained after being stirred for 24 h in the dark and were washed several times before being freeze dried. SiO_2-MB NPs (1 mg) were then mixed with 3 mL of ethanol and then 40 μL of APTS was added. The mixture was stirred in a 60 °C water bath for 3 hours. The obtained NH_2–SiO_2-MB NPs were purified by washing and centrifuging at 12 000 rpm. Finally, NH_2–SiO_2-MB NPs (10 mg) were suspended in Dox solution (2 mg mL^{-1}) overnight in the dark in order to absorb Dox on the particle surface/subsurface. They were then centrifuged to obtain NH_2–SiO_2-Dox/MB NPs.

MAb198.3 was attached to the Dox loaded NH_2–SiO_2-MB NPs using standard EDC–NHS coupling chemistry to obtain mAb198.3-SiO_2-Dox/MB NPs. The mole ratio of Dox loaded NH_2–SiO_2-MB : EDC : NHS : mAb198.3 = 1 : 5 : 5 : 10.

NH_2–SiO_2-Dox/MB NPs were analyzed by a UV-Vis spectrum (HitachiU-3501 UV–vis NIR spectrophotometer) to determine the amount of drug loading. The specific numbers are obtained based on the formula shown below.

$$\text{Drug encapsulation efficiency}(\%) = (\text{Amount of drug in nanoparticle})/(\text{Amount of drug input}) \times 100$$

$$\text{Drug loading efficiency}(\%) = (\text{Amount of drug in nanoparticle})/(\text{Amount of drug loaded nanoparticle}) \times 100$$

The drug encapsulation efficiencies of MB and Dox were estimated as 41.25%, and 63.69%, respectively, and their loading efficiencies were 12.13% and 14.99%, respectively.

TEM (PhilipsCM120) was employed for general morphology and size distribution characterization. Flow cytometry was used to investigate the mAb198.3-SiO_2-Dox/MB NPs' binding to colo-205 cells.

The binding of mAb198.3 to SiO_2-Dox/MB was examined by SDS-PAGE. In brief, approximately 0.5 mg of mAb198.3-SiO_2-Dox/MB or SiO_2-Dox/MB was centrifuged, and 40 μl of 2× SDS loaded buffer containing dithiothreitol (DTT) was added to the resulting pellet. They were boiled for 5 min before being separated by SDS-PAGE under reducing conditions using 12% polyacrylamide gel. Free mAb198.3 was taken as the control. The resolved proteins were stained using Coomassie Brilliant Blue.

Flow cytometry assay

The interaction of the mAb198.3-APC, or isotype antibody-APC, or mAb198.3-MB-SiO_2-Dox, or MB-SiO_2-Dox with Colo205 cells was analyzed using flow cytometry, in order to characterize the tumor cell binding *via* mAb198.3. Colo 205 cells were harvested and incubated with free mAb198.3-APC, or isotype antibody-APC, or mAb198.3-MB-SiO_2-Dox, or MB-SiO_2-Dox (20 μg ml^{-1}) for 30 min at 4 °C. After incubation, cells were washed three times and re-suspended in PBS. Samples were analyzed using a FACS Calibur flow cytometer and CellQuest™ Pro software (BD Bioscience, San Jose, CA). Each experiment was carried out in triplicate.

Characterization of the drug release and carrier decomposition process

The drug release profile of mAb198.3-SiO_2-Dox/MB NPs was determined by a UV-vis spectrum. Equal amounts of mAb198.3-SiO_2-Dox/MB NPs (1 mg mL^{-1}) were dispersed in 10 mL deionized water or Mes buffer (pH 5.5). Each sample was then divided into 12 equal groups. Each group was centrifuged at different time points and the supernatant was collected. The NPs were dried and re-dispersed in deionized water. UV-vis absorption spectra were taken from both re-dispersed particle solutions and supernatants using a Hitachi U-3501 UV-vis NIR spectrophotometer. The degradation of the SiO_2 carrier was monitored by morphology investigation using TEM.

We also examined the drug release profile of colo-205 cells, which were cultured in RPMI 1640 medium, supplemented with 10% heat-inactivated fetal bovine serum, 1% streptomycin, and 1% penicillin. The cells were maintained in a standard cell culture incubator at 37 °C under a humidified atmosphere with 5% CO_2. All of the NPs were sterilized *via* cobalt-60 (NPs in powder form) for 24 h and dispersed in the medium by ultra-sonication right before their introduction into the cells. Cells were seeded at initial densities of 5×10^4 cells per mL in 25 mm^2 flasks and incubated for 24 h, and the medium was changed to one with NPs. At different time points, cell samples were collected and washed with PBS. After that, the cells were treated with 0.1% Triton X-100 at 37 °C for 5 minutes for enhancing cell membrane permeability, then centrifuged (16 000*g*) to separate the released drug molecules

from the residual NPs (mainly existing as NP aggregates in the endo/lysosomes).

Cell viability characterization

The MTT assay was conducted to evaluate cell viability after various treatments. Colo-205 cells (50 000 cells per well) seeded in 96-well plates were cultured in RPMI1640 with 10% fetal bovine serum at 37 °C under 5% of CO_2 in an incubator. MB and Dox were diluted in a culture medium to obtain the desired concentrations (from 1 ng ml^{-1} to 1 mg ml^{-1}). The cell viability was determined using optical absorbance (490 nm) and an ELISA plate reader. The corresponding concentration of specific cell viability (Dox about 75% and MB about 90%) was chosen as the concentration for the following experiments.

Cell viabilities for the sequential administration of MB and Dox (Dox first, followed by MB) with different time lags between the two (from simultaneously to 20 h) at fixed drug concentrations (as defined above), or with NP treatment were also investigated by the MTT assay.

Antitumor efficacy evaluation *in vivo*

All animal experiments were approved by the Animal Experiment Administration Committee of the Fourth Military Medical University. Female BALB/C nude mice (6–8 weeks) were purchased from Hunan SJA Laboratory Animal Co., Ltd. Colo-205 cells (5×10^6 cells, total volume 0.1 mL) were injected into mice leg subcutaneously to establish tumors. When the diameters of tumors were above 0.2 cm as measured by calipers, the mice bearing tumors were randomly divided into 12 groups (5 mice per group): the saline control group and 11 treatment groups. Nanoparticles and drugs dissolved in saline were administered by a tail intravenous (iv) injection every 3 days at Dox doses of 5 mg kg^{-1} for 4 weeks. All animals were monitored for activity, physical condition, body weight, and tumor growth. The bodyweight of each mouse was measured and recorded every week until sacrifice. Mice were sacrificed after 4 weeks of treatment. Tumor masses were removed and weighed.

All of the data are reported as the means ± S.D. Comparisons were performed with a one-way analysis of variance (ANOVA) followed by Bonferroni's multiple comparison tests using GraphPad Prism 5.01 software. Significance was defined as $P < 0.05$.

Conclusions

Tumor-targeting and programmable chemotherapeutic delivery were demonstrated by designing mAb198.3-SiO_2-Dox/MB self-decomposable nanoparticle drugs. A significantly enhanced antitumor efficacy was achieved due to both the targeting function of mAb198.3 on the NP surface, and the programmed sequential release of chemotherapeutics (Dox and MB, with the latter serving as the sensitizer for the former), with the latter feature determined by the loading ratio of the two chemo drugs and independent of any external stimuli. Such a nanoparticle drug system was also found to largely reduce the system toxicity of individual chemotherapeutics.

Acknowledgements

This work was partially funded by grants from the National Natural Science Foundation of China no. 81201179, Postdoctoral Science Foundation of China, and Hongkong Scholarship.

References

1 C. M. Hu, S. Aryal and L. Zhang, Nanoparticle-assisted Combination Therapies for Effective Cancer Treatment, *Ther. Delivery*, 2010, **1**, 323–334.
2 G. Bonadonna, E. Brusamolino, P. Valagussa, A. Rossi, L. Brugnatelli, C. Brambilla, M. De Lena, G. Tancini, E. Bajetta, R. Musumeci, *et al.* Combination Chemotherapy as an Adjuvant Treatment in Operable Breast Cancer, *N. Engl. J. Med.*, 1976, **294**, 405–410.
3 J. Lehar, A. S. Krueger, W. Avery, A. M. Heilbut, L. M. Johansen, E. R. Price, R. J. Rickles, G. F. Short 3rd, J. E. Staunton, X. Jin, *et al.* Synergistic Drug Dombinations Tend to Improve Therapeutically Relevant Selectivity, *Nat. Biotechnol.*, 2009, **27**, 659–666.
4 L. C. Hull, D. Farrell and P. Grodzinski, Highlights of Recent Developments and Trends in Cancer Nanotechnology Research-view from NCI Alliance for Nanotechnology in Cancer, *Biotechnol. Adv.*, 2014, **32**, 666–678.
5 H. Chen, Y. Zhao, H. Wang, G. Nie and K. Nan, Co-delivery Strategies Based on Multifunctional Nanocarriers for Cancer Therapy, *Curr. Drug Metab.*, 2012, **13**, 1087–1096.
6 D. B. Pacardo, F. S. Ligler and Z. Gu, Programmable Nanomedicine Synergistic and Sequential Drug Delivery Systems, *Nanoscale*, 2015, **7**, 3381–3391.
7 S. Mitragotri, P. A. Burke and R. Langer, Overcoming the challenges in administering biopharmaceuticals: formulation and delivery strategies, *Nat. Rev. Drug Discovery*, 2014, **13**, 655–672.
8 S. W. Morton, M. J. Lee, Z. J. Deng, E. C. Dreaden, E. Siouve, K. E. Shopsowitz, N. J. Shah, M. B. Yaffe and P. T. Hammond, A nanoparticle-based combination chemotherapy delivery system for enhanced tumor killing by dynamic rewiring of signaling pathways, *Sci. Signaling.*, 2014, **7**, ra44.
9 N. S. Gandhi, R. K. Tekade and M. B. Chougule, Nanocarrier Mediated Delivery of SiRNA/miRNA in Combination with Chemotherapeutic Agents for Cancer Therapy: Current Progress and Advances, *J. Controlled Release*, 2014, **194**, 238–256.
10 V. P. Torchilin, Multifunctional, Stimuli-Sensitive Nanoparticulate Systems for Drug Delivery, *Nat. Rev. Drug Discovery*, 2014, **13**, 813–827.

11 E. K. Lim, E. Jang, K. Lee, S. Haam and Y. M. Huh, Delivery of Cancer Therapeutics Using Nanotechnology, *Pharmaceutics*, 2013, **5**, 294–317.
12 J. Gao, W. Zhong, J. He, H. Li, H. Zhang, G. Zhou, B. Li, Y. Lu, H. Zou, G. Kou, *et al.* Tumor-Targeted PE38KDEL Delivery via PEGylated Anti-HER2 Immunoliposomes, *Int. J. Pharm.*, 2009, **374**, 145–152.
13 K. B. Sutradhar and M. L. Amin, Nanotechnology in Cancer Drug Delivery and Selective Targeting, *ISRN Nanotechnol.*, 2014, **2014**, 1–12.
14 K. Park, Nanotechnology: What It Can Do for Drug Delivery, *J. Controlled Release*, 2007, **120**, 1–3.
15 Y. Li and L. Yang, Driving Forces for Drug Loading in Drug Carriers, *J. Microencapsulation*, 2015, **3**, 1–18.
16 H. J. Hah, G. Kim, Y. K. Lee, D. A. Orringer, O. Sagher, M. A. Philbert and R. Kopelman, Methylene Blue-Conjugated Hydrogel Nanoparticles and Tumor-CellTargeted Photodynamic Therapy, *Macromol. Biosci.*, 2011, **11**, 90–99.
17 W. M. Sharman, C. M. Allen and J. E. van Lier, Photodynamic therapeutics: basic principles and clinical applications, *Drug Discovery Today*, 1999, **4**, 507–517.
18 H. Mohr, B. Lambrecht and A. Selz, Photodynamic Virus Inactivation of Blood Components, *Immunol. Invest.*, 1995, **24**, 73–85.
19 H. Mohr, B. Lambrecht and H. Schmitt, German Red Cross Blood Transfusion Service Lower Saxony, Institute Springe, *Dev. Biol. Stand.*, 1993, **81**, 177–183.
20 S. J. Wagner, D. Robinette, J. Storry, X. Y. Chen, J. Shumaker and L. Benade, Differential sensitivities of viruses in red cell suspensions to methylene blue photosensitization, *Transfusion*, 1994, **34**, 521–526.
21 A. J. Matisoff and M. K. Panni, Methylene blue treatment for methemoglobinemia and subsequent dramatic bispectral index reduction, *Anesthesiology*, 2006, **105**, 228.
22 P. Ma and R. J. Mumper, Anthracycline Nano-Delivery Systems to Overcome Multiple Drug Resistance: A Comprehensive Review, *Nano Today*, 2013, **8**, 313–331.
23 S. Zhang, Z. Chu, C. Yin, C. Zhang, G. Lin and Q. Li, Controllable Drug release and Simultaneously Carrier Decomposition of SiO_2-Drug Composite Nanoparticles, *J. Am. Chem. Soc.*, 2013, **135**, 5709–5716.
24 J. Legault, P. L. Larouche, I. Cote, L. Bouchard, A. Pichette, B. H. Robinson and C. Morin, Low-Concentration Methylene Blue Maintains Energy Production and Strongly Improves Survival of Leigh Syndrome French Canadian Skin Fibroblasts, *J. Pharm. Pharm. Sci.*, 2011, **14**, 438–449.
25 P. Pileri, S. Campagnoli, A. Grandi, M. Parri, E. D. Camilli, C. Song, I. Naldi, P. Sarmientos, C. Cinti, B. Jin, G. Grandi, G. Viale, L. Terracciano and R. Grifantini, FAT1: a target for monoclonal antibody therapy in colon cancer. Submitted.